

# Leaf photosynthesis is positively correlated with xylem and phloem areas in leaf veins in rice (*Oryza sativa*) plants

Guanjun Huang, Yu Shu, Shaobing Peng and Yong Li\*<sup>✉</sup>

National Key Laboratory of Crop Genetic Improvement, Ministry of Agriculture Key Laboratory of Crop Ecophysiology and Farming System in the Middle Reaches of the Yangtze River, College of Plant Science and Technology, Huazhong Agricultural University, Wuhan, Hubei, China

\* For correspondence. E-mail [liyong@mail.hzau.edu.cn](mailto:liyong@mail.hzau.edu.cn)

Received: 16 November 2021 Returned for revision: 5 January 2022 Editorial decision: 7 February 2022 Accepted: 9 February 2022  
Electronically published: 10 February 2022

- **Background and Aims** Leaf structure is an important determinant of leaf photosynthesis; however, the impacts of leaf structural traits on gas exchange parameters are still not fully understood. In the present study, 11 rice genotypes were grown in pots to investigate the influence of leaf structural traits on leaf photosynthesis and hydraulic conductance ( $K_{\text{leaf}}$ ).
- **Methods** In this study, leaf photosynthetic rate ( $A$ ), stomatal conductance ( $g_s$ ), mesophyll conductance and  $K_{\text{leaf}}$  were measured. In addition, leaf structural traits including leaf thickness (LT), leaf mass per area and leaf xylem and phloem sizes were also measured to investigate their impacts on rice photosynthesis.
- **Key Results** We found that the total area of xylem conduits per major vein ( $X_{\text{major}}$ ), leaf phloem area per minor vein ( $P_{\text{minor}}$ ) and LT were positively correlated with  $K_{\text{leaf}}$ ,  $g_s$  and  $A$ . The path analysis suggested that, however, only  $P_{\text{minor}}$  had a direct impact on  $A$ ;  $X_{\text{major}}$  had an indirect impact on  $A$  via  $g_s$  and  $P_{\text{minor}}$ , while LT did not show any direct or indirect impact on  $A$ .
- **Conclusion** This study highlighted the importance of manipulations in  $X_{\text{major}}$  and  $P_{\text{minor}}$ , two previously overlooked leaf traits, to improve leaf photosynthesis in rice plants.

**Key words:** Photosynthesis, xylem size, phloem size, leaf hydraulic conductance, leaf thickness, stomatal conductance, mesophyll conductance.

## INTRODUCTION

CO<sub>2</sub> diffusion capacity from ambient atmosphere to carboxylation sites, including stomatal conductance ( $g_s$ ) and mesophyll conductance ( $g_m$ ), is the major limitation for photosynthesis (Flexas *et al.*, 2013, 2021).  $g_s$  is generally determined by stomatal density, size and aperture. Stomatal aperture is usually determined by leaf water transport capacity, defined as leaf hydraulic conductance ( $K_{\text{leaf}}$ ), because adequate water supply to guard cells is needed to support transpirational water loss (Buckley, 2005; Xiong *et al.*, 2015, 2017). The impacts of stomatal size and density on  $g_s$  have been well documented in previous studies (Franks and Farquhar, 2007; Franks and Beerling, 2009). However, the water transport process inside leaves and its impacts on stomatal aperture are not fully understood.

Water transport through leaves follows two pathways that operate in series. Water first flows through leaf xylem conduits and then through tissues outside the xylem. Leaf vein density has been suggested to be the most important leaf trait determining  $K_{\text{leaf}}$ , because a high leaf vein density could both increase the parallel pathways for water diffusion through xylem conduits and shorten the transport distance from xylem conduits to stomata (Boyce *et al.*, 2009; Brodribb, 2009; Buckley *et al.*, 2015; Scoffoni *et al.*, 2016). However, leaf vein density has frequently been found not to correlate with  $K_{\text{leaf}}$  or  $g_s$  (Flexas *et al.*, 2013;

Xiong *et al.*, 2015, 2017). In addition to leaf vein density, the area of xylem conduits should be an important determinant to hydraulic conductance through the xylem ( $K_x$ ) and in turn to  $K_{\text{leaf}}$  (Nardini *et al.*, 2005; Sack and Frole, 2006; McKown *et al.*, 2010; Sack and Scoffoni, 2013). Unfortunately, the experimental evidence regarding the relationships between xylem conduit area per leaf vein and  $K_{\text{leaf}}$ ,  $g_s$  and leaf photosynthetic rate ( $A$ ) is still lacking in rice plants (Xiong *et al.*, 2015, 2017). We hypothesized that xylem conduit area per leaf vein is positively correlated with  $K_{\text{leaf}}$ , and in turn with  $g_s$  and  $A$ . Therefore, the first objective of this study was to investigate the impact of xylem conduits per leaf vein on  $K_{\text{leaf}}$  and gas exchange parameters in one of the most important cereals, rice (*Oryza sativa*) plants.

In addition to CO<sub>2</sub> diffusion capacity and leaf biochemistry, the transport capacity of carbohydrates is a key determinant of leaf photosynthesis (Sharkey, 1985). Leaf photosynthesis is severely suppressed when photoassimilates cannot be efficiently exported from the source leaves (Krapp and Stitt, 1995; Ainsworth and Bush, 2011; Sugiura *et al.*, 2020). The transport capacity of carbohydrates is reported to be closely related to leaf vein density and phloem infrastructure (Flora and Madore, 1996; Ainsworth and Bush, 2011; Stewart *et al.*, 2019). Leaf photosynthetic rate has been found to be positively correlated to total phloem cross-sectional area per leaf vein (Adams *et al.*, 2007, 2013, 2016). However, these studies were mainly

conducted across different plant species, and such a study in a single species is lacking. We hypothesized that leaf phloem area per leaf vein is also positively correlated with  $A$  in a single plant species. Therefore, the second objective of this study was to investigate the correlation between leaf phloem area per leaf vein and gas exchange parameters in rice plants.

The co-ordination of development in leaf structures has frequently been found in previous studies, and leaf thickness (LT) is positively correlated with xylem diameter and bundle sheath cell area among species (Brodrribb *et al.*, 2013; John *et al.*, 2013). As an important leaf structural trait determining leaf photosynthesis, LT has usually been found to be positively related to  $A$  (Hanba *et al.*, 1999, 2002; Xiong *et al.*, 2015; Han *et al.*, 2019). The higher photosynthetic rate in thicker leaves is usually associated with higher leaf nitrogen content, larger mesophyll surface area, greater  $g_m$  and/or  $K_{leaf}$  among and/or within plant species. However, the correlation between LT and gas exchange parameters found previously may relate to the co-ordination between leaf structures. Therefore, we hypothesized that LT is correlated with the size of leaf xylem and phloem, and thus with gas exchange parameters in rice plants. Therefore, the third objective of our study was to investigate the relationships between LT and total area of xylem conduits and phloem area per leaf vein, and to study the impacts of leaf thickness on  $K_{leaf}$  and  $A$  in rice plants.

Leaf mass per area (LMA) is an important leaf trait, which is closely related to leaf physiological and structural parameters. The correlation between LMA and  $A$  is inconsistent in previous studies (Hassiotou *et al.*, 2010; Lu *et al.*, 2020; Reddy *et al.*, 2020; Ye *et al.*, 2020). It has been hypothesized that the relationship between LMA and  $A$  is linked to the contributions of LT and leaf density (LD) to LMA (Niinemets, 1999; Poorter *et al.*, 2009). The LMA may be positively correlated with  $A$  if the variation of LMA is determined by LT as previously mentioned. In contrast, LMA may be negatively correlated with  $A$  if LD determines the variation of LMA, because non-photosynthetic components are more densely packed than photosynthetic components (Niinemets, 1999; Poorter *et al.*, 2009). Therefore, the fourth objective of our study was to investigate the relationships between LMA and LT, and thus  $A$ .

In the present study, 11 rice genotypes were grown in pots outdoors. The objectives were to investigate the influences of leaf structural traits, including total area of xylem conduits and phloem area per leaf vein, LT and LMA on  $K_{leaf}$  and gas exchange parameters. The findings may provide some novel information for crop breeding because improving photosynthesis is considered as the most promising approach to further boost crop yield in the future (Zhu *et al.*, 2010; Long *et al.*, 2015).

## MATERIALS AND METHODS

### Plant material and growth conditions

Eleven rice (*Oryza sativa* L.) genotypes (Supplementary data Table S1) were grown in pots outdoors under natural sunlight in Huazhong Agricultural University, Wuhan, China. Three seedlings were grown per pot in 13 L pots filled with 10 kg of soil, and 10 g of compound fertilizer (N:P<sub>2</sub>O<sub>5</sub>:K<sub>2</sub>O = 16:16:16 %) was applied by mixing into the soil. A minimum water layer of 2 cm

above the soil surface was maintained in order for all plants to avoid drought stress. The soil used in this study had the following properties: pH 7.1, 6.7 g kg<sup>-1</sup> of organic matter, 6.27 mg kg<sup>-1</sup> of Olsen-P, 129 mg kg<sup>-1</sup> of exchangeable K and 0.63 ‰ total N. Measurements were conducted on the most recently fully expanded leaves at the illering stage from 45 d after emergence.

### Measurements of leaf gas exchange parameters

Leaf gas exchange parameters and carbon isotope compositions of CO<sub>2</sub> were measured using a Li-Cor 6800 (LI-COR Inc., Lincoln, NE, USA) coupled to a Tunable Diode Laser Absorption Spectrometer (TDL, TGA200A; Campbell Scientific Inc., Logan, UT, USA). The Li-Cor 6800 was fitted with a 6 × 6 cm leaf chamber (Li6800-13) and a red–green–blue light source (Li6800-03). In this study, two leaves were placed in the leaf chamber during each measurement. Light intensity inside the leaf chamber was set to 1500 μmol m<sup>-2</sup> s<sup>-1</sup> and the light quality was set to 10:90 of blue:red light. Leaf temperature was controlled at 25 °C, and the CO<sub>2</sub> concentration surrounding the leaf was maintained at 400 μmol mol<sup>-1</sup> with a CO<sub>2</sub> mixer. The flow rate through the leaf chamber was maintained at 350–700 μmol s<sup>-1</sup> and the relative humidity was set to 60 %. Excess flow from the leaf chamber vented at the valve before the TDL. The measurements of gas exchange and isotope compositions were conducted within an environment-controlled room. The temperature in the room was controlled using an air conditioner to match the desired leaf temperature, and air humidity was about 60 % during the experiment. The whole plants were illuminated using LED lights, and the light intensity at the leaf level was 1200 μmol m<sup>-2</sup> s<sup>-1</sup> in the room.

Mesophyll conductance was calculated according to Barbour *et al.* (2016) and included the ternary effects of transpiration rate on the flux of isotopologues of CO<sub>2</sub> through the stomata (Farquhar and Cernusak, 2012).  $g_m$  was calculated from the difference between the calculated carbon isotope discrimination, assuming infinite  $g_m$  ( $\Delta^{13}C_i$ ), and the data were measured by the coupled system ( $\Delta^{13}C_{obs}$ ).

$$\Delta^{13}C_i = \frac{1}{1-t} \left[ a_b \frac{C_a - C_s}{C_a} + a_s \frac{C_s - C_i}{C_a} \right] + \frac{1+t}{1-t} \left[ b \frac{C_i}{C_a} - \frac{\alpha_b}{\alpha_{e'}} e' \frac{R_d}{A + R_d} \frac{C_i - \Gamma^*}{C_a} - \frac{\alpha_b}{\alpha_f} f \frac{\Gamma^*}{C_a} \right] \quad (1)$$

$C_a$ ,  $C_s$  and  $C_i$  represent the ambient, leaf surface and intercellular CO<sub>2</sub> concentration, respectively;  $a_b$ , the fractionation occurring during CO<sub>2</sub> diffusion through the boundary layer (0.0029; Evans *et al.*, 1986);  $a_s$ , the fractionation occurring during CO<sub>2</sub> diffusion through the stomata (0.0044; Farquhar and Richards, 1984);  $b$ , the fractionation during carboxylation (0.03; Guy *et al.*, 1993);  $e'$ , the fractionation during day respiration (−0.003; Tcherkez *et al.*, 2010);  $f$ , the fractionation during photorespiration (0.0162; Evans and von Caemmerer, 2013);  $\alpha_b$ , the fractionation factor for carboxylation (1 +  $b$ );  $\alpha_{e'}$ , the fractionation factor for day respiration (1 +  $e'$ );  $\alpha_f$ , the fractionation factor for photorespiration (1 +  $f$ );  $R_d$  represents the day respiration;  $\Gamma^*$  represents the CO<sub>2</sub> compensation point in the

absence of  $R_d$ ; and  $t$  is the ternary effect.  $t$  is given by the following equation

$$t = \frac{\alpha_{ac} E}{2g_{ac}} \quad (2)$$

$\alpha_{ac}$  represents the fractionation factor of  $\text{CO}_2$  diffusion ( $1 + \bar{a}$ ),  $g_{ac}$  represents the total conductance of  $\text{CO}_2$  through the boundary layer and stomata.  $\bar{a}$  represents the weighted fractionation across the boundary layer and stomata and is given by (Evans *et al.*, 1986)

$$\bar{a} = \frac{a_b(C_a - C_s) + a_s(C_s - C_i)}{C_a - C_i} \quad (3)$$

Mesophyll resistance ( $r_m$ ) can then be calculated from the difference between  $\Delta^{13}\text{C}_i$  and  $\Delta^{13}\text{C}_{obs}$  following Farquhar and Cernusak (2012) and Barbour *et al.* (2016).

$$r_m = \frac{1-t}{1+t} (\Delta^{13}\text{C}_i - \Delta^{13}\text{C}_{obs}) \frac{C_a}{A \left( b - a_m - \frac{\alpha_b}{\alpha_e} e' \frac{R_d}{A+R_d} \right)} \quad (4)$$

where  $r_m$  is the reciprocal of  $g_m$ ,  $g_m = (1/r_m)$ . The values of  $F^*$  and  $R_d$  at 25 °C were used following Bernacchi *et al.* (2002).

#### Measurement of leaf hydraulic conductance

Leaf hydraulic conductance was measured in an environment-controlled room using the evaporative flux method (Sack and Scoffoni, 2012) and all plants were dark-adapted overnight before measurement. The excised leaves (4–8 leaves per genotype) were placed under LED lights for transpiration; the light intensity at the leaf level was  $1500 \mu\text{mol m}^{-2} \text{s}^{-1}$  and the air temperature of room was controlled at 25 °C. The leaf temperature was measured using a Multi-Channel Digital Thermometer (AZ88598, AZ Instrument Corp. Ltd, Taichung, China) and was found to be slightly higher than the air temperature because of the heating effect of the lights; the average leaf temperature was  $27.4 \pm 0.6$  °C across genotypes during the measurement of  $K_{leaf}$ . When the leaf transpiration rate had reached a steady state for at least 15 min, the leaves were immediately detached and placed in a sealable bag which had previously had the air removed. After equilibration for at least 15 min,  $\Psi_{leaf}$  was measured using a pressure chamber (PMS Instrument Company, Albany, OR, USA).  $K_{leaf}$  was calculated as

$$K_{leaf} = \frac{E}{\Psi_{water} - \Psi_{leaf}} \quad (5)$$

where  $\Psi_{water}$  is the water potential of distilled water, which is 0 MPa in the present study. It should be noted that guttation was observed in YY12 and YY2640 after dark adaptation overnight, while it was not found in other genotypes.

#### Measurements of leaf mass per area

The newly expanded leaves were detached and photographed. The images were used to measure the leaf area using ImageJ (Wayne Rasband/NIH, Bethesda, MD, USA). The leaves were then oven-dried to achieve a constant weight at 80 °C, and the leaf dry mass was measured. The LMA was calculated as the ratio of leaf dry mass to leaf fresh area.

#### Measurements of leaf structural traits

After the gas exchange measurements, three leaf discs (1–2 cm<sup>2</sup>) from different seedlings were collected and quickly fixed in formalin–acetic acid–methanol; they were then dehydrated in an ethanol series, embedded in Paraplast, and sectioned at 5  $\mu\text{m}$  using a microtome (Leica HistoCore, Leica Microsystems, Nussloch, Germany). The sections were deparaffinized through two changes of 100 % EGEEA for 10–15 min each, two changes of 100 % ethanol for 10 min each and 95, 90 and 80 % ethanol for 10 min each. Then, the segments were washed in water. After that, they were stained in 1 % diluted Safranin for 3–5 s, followed by flushing in tap water. The segments were then decoloured through 50, 70 and 80 % ethanol washes for 3–8 s each. Following a colouration in 0.5 % quick green and 95 % ethanol for 4–6 s, the segments were put in three successive washes of 100 % ethanol for 5, 10 and 30 s, individually. They were then drenched in xylene for 5 min and mounted with a permanent resin. Leaf structures were photographed at a magnification of  $\times 400$  with a Nikon Eclipse E100 light microscope (Nikon Optical, Tokyo, Japan). The LT and LD were calculated using the light microscope images with ImageJ:

$$LT = \frac{\text{Area of cross section}}{\text{Width of cross section}} \quad (6)$$

$$LD = \frac{LMA}{LT} \quad (7)$$

Rice leaf veins can be categorized into three types based on their size: midrib, major veins and minor veins (Supplementary data Fig. S1). In the present study, the total area of xylem conduits and phloem area per major vein ( $X_{major}$  and  $P_{major}$ ), total area of xylem conduits and phloem area per minor vein ( $X_{minor}$  and  $P_{minor}$ ), total vascular bundle areas per major and per minor veins ( $S_{major}$  and  $S_{minor}$ ) and interveinal distance between major veins and between minor veins ( $IVD_{major}$  and  $IVD_{minor}$ ) were directly measured from leaf cross-sections. There were in total three different leaf cross-sections from three different plants for each genotype and at least 3–5 technical replicates in each cross-section for all parameters.

#### Measurements of stomatal morphologies

In order to study whether intraspecific variation of  $g_s$  in rice plants is related to stomatal morphologies, stomatal size (SZ) and stomatal density (SD) were estimated. Three small leaf discs (approx.  $5 \times 5$  mm) from the centre of each leaf (avoiding the midrib) were placed with the fixative 2.5 % glutaric aldehyde in  $0.1 \text{ mol l}^{-1}$  phosphate buffer (pH 7.6). The leaf samples were stored at 4 °C until investigation. For each genotype, three leaves from different plants were chosen. Four pictures of both the abaxial and adaxial sides were taken, utilizing a scanning electron microscope (JSM-6390LV, Tokyo, Japan) under vacuum conditions. The SD, guard cell length (L) and guard cell width (W) on each leaf side were estimated with. In this study, SZ was determined based on the assumption that stomata are elliptical in shape



with their major axis equivalent to L and their minor axis equivalent to W (Zhang *et al.*, 2019):

$$SZ = \frac{L}{2} \times \frac{W}{2} \times \pi \quad (8)$$

### Statistical analysis

Multivariate analysis of variance (MANOVA) was used to assess the difference in measured traits (Tables 1 and 2) among the tested rice genotypes using SPSS 20. Both linear and non-linear correlations were analysed using Sigma Plot 12.5 (SPSS Inc., Chicago, IL, USA), and the regressions with the lowest residual sum of squares are shown. In order to investigate whether and how the correlations between specific traits and  $A$  depend on other variables, a partial correlative analysis was applied using SPSS 20 (Table 3), which could remove the effect of a specific trait on  $A$  when studying the correlations between  $A$  and other traits.

The interactions between leaf photosynthesis and leaf structural and physiological traits were further analysed by path analysis to investigate which parameters determined the variation of  $A$  among rice genotypes in our study. Path analysis was tested using the R package lavaan based on genotype mean values, which were  $\log_{10}$  transformed before analysis. We fitted each candidate model using a Wishart likelihood (Wishart, 1928), which can compensate for any remaining non-normality in the data. The minimal adequate model was reported according to the following criteria: non-significant  $\chi^2$  tests ( $P > 0.05$ ), low root mean square error of approximation index (RMSEA  $< 0.05$ ), high Tucker–Lewis index (TLI  $\geq 0.90$ ) and comparative fit index (CFI  $\geq 0.90$ ) (Grace *et al.*, 2010).

## RESULTS

### Variations in leaf gas exchange, hydraulic and structural traits

In general, there were large variations in leaf gas exchange and hydraulic traits among the studied rice genotypes (Table 1). The variations in  $A$ ,  $g_m$  and  $g_s$  were similar, and varied by approx. 1.5-fold among the studied genotypes (Table 1). A larger

variation was observed in  $K_{leaf}$ , from  $12.2 \pm 2.6$  mmol m<sup>-2</sup> s<sup>-1</sup> MPa<sup>-1</sup> in YLY6 to  $78.3 \pm 12.7$  mmol m<sup>-2</sup> s<sup>-1</sup> MPa<sup>-1</sup> in YY2640 (Table 1). However,  $C_i$  and  $C_c$  did not show significant variation among genotypes (Table 1).

There were also significant intraspecific variations in leaf structural traits (Table 2). The largest variation was found in  $X_{minor}$ , which varied from  $54 \pm 14$  to  $187 \pm 74$   $\mu\text{m}^2$  among genotypes. There were large variations in  $X_{major}$ ,  $P_{major}$ ,  $P_{minor}$ ,  $S_{major}$  and  $S_{minor}$ , of 2.10-, 1.90-, 2.08-, 1.89- and 2.15-fold, respectively, among the studied genotypes (Table 2). The variations in LMA, LT and LD were similar, differing by 1.47-, 1.63- and 1.44-fold, respectively (Table 2). The least variations among genotypes were found in  $IVD_{major}$  and  $IVD_{minor}$ , which were changed by 1.32- and 1.25-fold, respectively (Table 2). Substantial differences were also observed in stomatal size and density, which varied between 1.32- and 1.81 fold among genotypes (Table 2).

### Relationships between leaf gas exchange, hydraulic and structural traits

In the present study,  $A$  was positively correlated with  $g_s$ ,  $g_m$  and  $K_{leaf}$  (Fig. 1), but it was not correlated with either  $C_i$  or  $C_c$  (Supplementary data Fig. S2). In addition, we found that  $X_{major}$  and  $X_{minor}$  were positively correlated with  $g_s$ ,  $g_m$ ,  $K_{leaf}$  and  $A$  (Fig. 2), except for the non-significant relationship between  $X_{minor}$  and  $g_m$  (Fig. 2B). Similarly,  $P_{major}$  and  $P_{minor}$  were positively correlated with  $g_s$ ,  $K_{leaf}$  and  $A$  (Fig. 3), but they were not significantly correlated with  $g_m$  (Fig. 3B). Additionally, we also observed that  $S_{major}$  and  $S_{minor}$  were positively correlated with  $g_s$ ,  $g_m$ ,  $K_{leaf}$  and  $A$  (Supplementary data Fig. S3), though no significant relationship was found between  $S_{minor}$  and  $g_m$  (Supplementary data Fig. S3f). There was no significant relationship between  $IVD$  and  $g_s$ ,  $g_m$ ,  $K_{leaf}$  or  $A$  (Supplementary data Fig. S4).

In this study,  $g_s$  was positively correlated with  $K_{leaf}$  among rice genotypes (Fig. 4), while it was not correlated with either stomatal size or density (Supplementary data Fig. S5). The LT and LMA were found to be positively correlated with  $g_s$ ,  $K_{leaf}$  and  $A$ ; however,  $g_m$  was only positively correlated with LMA and not with LT (Figs 5 and 6). There was no significant relationship between LD and  $g_s$ ,  $g_m$ ,  $K_{leaf}$  or  $A$  (data not shown).

TABLE 1. The intraspecific variations in leaf photosynthetic rate ( $A$ ), mesophyll conductance ( $g_m$ ), stomatal conductance ( $g_s$ ), intercellular  $\text{CO}_2$  concentration ( $C_i$ ), chloroplast  $\text{CO}_2$  concentration ( $C_c$ ) and leaf hydraulic conductance ( $K_{leaf}$ ) in the 11 studied rice genotypes

Genotype	$A$ ( $\mu\text{mol m}^{-2} \text{s}^{-1}$ )	$g_m$ ( $\text{mol m}^{-2} \text{s}^{-1}$ )	$g_s$ ( $\text{mol m}^{-2} \text{s}^{-1}$ )	$C_i$ ( $\mu\text{mol mol}^{-1}$ )	$C_c$ ( $\mu\text{mol mol}^{-1}$ )	$K_{leaf}$ ( $\text{mmol m}^{-2} \text{s}^{-1} \text{MPa}^{-1}$ )
LYPJ	29.3 $\pm$ 2.4	0.60 $\pm$ 0.01	0.57 $\pm$ 0.04	317 $\pm$ 6	269 $\pm$ 10	17.4 $\pm$ 4.7
TYHZ	32.9 $\pm$ 3.0	0.71 $\pm$ 0.09	0.80 $\pm$ 0.04	334 $\pm$ 8	287 $\pm$ 16	18.4 $\pm$ 2.9
YY673	28.9 $\pm$ 3.5	0.52 $\pm$ 0.13	0.56 $\pm$ 0.05	318 $\pm$ 3	261 $\pm$ 4	17.8 $\pm$ 4.8
YLY2	34.0 $\pm$ 2.5	0.70 $\pm$ 0.08	0.75 $\pm$ 0.13	326 $\pm$ 8	278 $\pm$ 9	19.3 $\pm$ 6.2
YY12	37.5 $\pm$ 0.7	0.74 $\pm$ 0.02	0.85 $\pm$ 0.10	329 $\pm$ 8	278 $\pm$ 7	49.2 $\pm$ 14.2
FLYX1	29.8 $\pm$ 1.3	0.57 $\pm$ 0.05	0.61 $\pm$ 0.03	322 $\pm$ 1	269 $\pm$ 3	21.9 $\pm$ 5.3
HY3	26.3 $\pm$ 3.3	0.49 $\pm$ 0.13	0.58 $\pm$ 0.23	322 $\pm$ 21	266 $\pm$ 29	18.8 $\pm$ 3.8
YY2640	38.3 $\pm$ 2.7	0.65 $\pm$ 0.02	0.85 $\pm$ 0.26	324 $\pm$ 17	265 $\pm$ 15	78.3 $\pm$ 12.7
SY63	30.8 $\pm$ 3.3	0.63 $\pm$ 0.11	0.65 $\pm$ 0.13	323 $\pm$ 10	273 $\pm$ 13	20.0 $\pm$ 3.3
YLY6	30.1 $\pm$ 1.2	0.53 $\pm$ 0.06	0.58 $\pm$ 0.08	316 $\pm$ 11	258 $\pm$ 5	12.2 $\pm$ 2.6
N22	31.5 $\pm$ 0.8	0.52 $\pm$ 0.02	0.70 $\pm$ 0.03	327 $\pm$ 5	267 $\pm$ 5	16.1 $\pm$ 5.6
MANOVA	$P < 0.001$	$P < 0.01$	$P < 0.05$	$P = 0.639$	$P = 0.341$	$P < 0.001$

Data are shown as means  $\pm$  s.d. of 3–5 biological replicates for  $A$ ,  $g_m$ ,  $g_s$ ,  $C_i$  and  $C_c$ , and of 4–8 biological replicates for  $K_{leaf}$ .

TABLE 2. The intraspecific variations in leaf structural traits with means ± s.d. of three biological replicates in 11 rice genotypes

Genotype	LMA (g m <sup>-2</sup> )	LT (mm)	LD (mg cm <sup>-3</sup> )	IVD <sub>major</sub> (μm)	IVD <sub>minor</sub> (μm)	X <sub>major</sub> (μm <sup>2</sup> )	X <sub>minor</sub> (μm <sup>2</sup> )	P <sub>major</sub> (μm <sup>2</sup> )	P <sub>minor</sub> (μm <sup>2</sup> )	S <sub>major</sub> (μm <sup>2</sup> )	S <sub>minor</sub> (μm <sup>2</sup> )	SZ <sub>da</sub> (μm <sup>2</sup> )	SD <sub>da</sub> (mm <sup>2</sup> )	SD <sub>ab</sub> (mm <sup>2</sup> )	
LYPJ	35.5 ± 0.6	0.107 ± 0.013	0.334 ± 0.036	1532 ± 220	243 ± 26	2829 ± 355	69 ± 32	1765 ± 289	567 ± 118	8512 ± 1224	741 ± 80	68 ± 11	78 ± 20	448 ± 102	577 ± 68
TYHZ	45.7 ± 4.4	0.095 ± 0.008	0.483 ± 0.044	1462 ± 119	223 ± 16	3518 ± 605	87 ± 20	1816 ± 270	524 ± 99	9486 ± 1451	725 ± 107	66 ± 12	79 ± 19	557 ± 68	499 ± 47
YY673	40.5 ± 3.4	0.097 ± 0.008	0.421 ± 0.039	1350 ± 70	223 ± 11	2722 ± 329	87 ± 22	1560 ± 223	575 ± 106	7429 ± 773	699 ± 81	78 ± 13	88 ± 19	519 ± 51	581 ± 102
YLY2	50.4 ± 4.0	0.108 ± 0.011	0.472 ± 0.048	1418 ± 184	230 ± 20	3660 ± 520	102 ± 46	2187 ± 261	639 ± 107	10275 ± 1632	856 ± 168	78 ± 15	71 ± 12	420 ± 107	537 ± 52
YY12	48.9 ± 6.0	0.133 ± 0.011	0.371 ± 0.028	1583 ± 103	269 ± 14	4611 ± 740	150 ± 42	2470 ± 306	937 ± 96	12178 ± 1234	1157 ± 261	77 ± 12	86 ± 18	441 ± 70	548 ± 96
FLYX1	45.1 ± 5.3	0.110 ± 0.012	0.413 ± 0.048	1200 ± 145	215 ± 7	3236 ± 231	88 ± 17	1932 ± 242	499 ± 101	8796 ± 1103	832 ± 102	72 ± 15	75 ± 14	433 ± 54	504 ± 88
HY3	39.6 ± 3.9	0.099 ± 0.010	0.403 ± 0.042	1391 ± 134	218 ± 13	2737 ± 474	59 ± 10	1906 ± 256	542 ± 91	7314 ± 1011	744 ± 131	68 ± 15	75 ± 12	348 ± 84	510 ± 132
YY2640	52.2 ± 4.2	0.155 ± 0.015	0.340 ± 0.038	1459 ± 114	239 ± 11	5537 ± 485	187 ± 74	2967 ± 279	1038 ± 127	13820 ± 1036	1355 ± 244	85 ± 14	112 ± 20	462 ± 73	570 ± 72
SY63	39.6 ± 3.8	0.095 ± 0.009	0.418 ± 0.041	1523 ± 112	229 ± 23	2633 ± 430	66 ± 35	1733 ± 196	522 ± 128	8024 ± 943	629 ± 159	96 ± 13	73 ± 11	307 ± 60	440 ± 77
YLY6	42.6 ± 3.8	0.100 ± 0.021	0.443 ± 0.089	1423 ± 217	239 ± 23	2924 ± 908	54 ± 14	1819 ± 386	585 ± 128	7683 ± 2740	762 ± 176	60 ± 6	69 ± 10	517 ± 49	563 ± 116
N22	40.4 ± 2.0	0.106 ± 0.009	0.384 ± 0.031	1364 ± 159	222 ± 13	3291 ± 471	132 ± 59	1622 ± 187	579 ± 82	8810 ± 869	943 ± 160	72 ± 15	76 ± 10	399 ± 82	488 ± 65
MANOVA	P = 0.001	P < 0.001	P < 0.01	P < 0.001	P < 0.05	P < 0.001	P < 0.01	P < 0.001	P < 0.001	P < 0.001	P = 0.001	P < 0.001	P < 0.001	P < 0.001	P < 0.001

LMA, leaf mass per area; LT, leaf thickness; LD, leaf density; IVD<sub>major</sub>, interveinal distance between major veins; IVD<sub>minor</sub>, interveinal distance between minor veins; X<sub>major</sub>, total area of xylem conduits per major vein; X<sub>minor</sub>, total area of xylem conduits per minor vein; P<sub>major</sub>, phloem area per major vein; P<sub>minor</sub>, phloem area per minor vein; S<sub>major</sub>, vascular bundle area of major vein; S<sub>minor</sub>, vascular bundle area of minor vein; SZ<sub>da</sub>, stomatal size on leaf abaxial surface; SZ<sub>ad</sub>, stomatal size on leaf adaxial surface; SD<sub>da</sub>, stomatal density on leaf abaxial surface; and SD<sub>ad</sub>, stomatal density on leaf adaxial surface.

Relationships between A and leaf structural and physiological traits

In order to investigate whether the correlations between A and leaf structural and physiological traits are dependent on other variables, a partial correlative analysis was conducted (Table 3). There were significantly positive zero-order relationships between A and g<sub>m</sub>, g<sub>s</sub>, K<sub>leaf</sub>, X<sub>major</sub>, X<sub>minor</sub>, P<sub>major</sub>, P<sub>minor</sub> and LT. When g<sub>s</sub> was controlled, however, the relationships between A and g<sub>m</sub>, K<sub>leaf</sub>, X<sub>minor</sub> and P<sub>major</sub> were not significant, and the r values of X<sub>major</sub>-A, P<sub>minor</sub>-A and LT-A correlations were greatly decreased. When X<sub>major</sub> was controlled, the correlations between A and K<sub>leaf</sub>, X<sub>minor</sub>, P<sub>major</sub>, P<sub>minor</sub> and LT were not significant, but the correlations between A and g<sub>m</sub> and g<sub>s</sub> were significant. In fact, the correlations between A and g<sub>s</sub> and X<sub>major</sub> were all significant regardless of the controlled traits. This suggested that g<sub>s</sub> and X<sub>major</sub> are two major determinants of A in this study (Table 3).

To identify the direct and indirect effects of leaf structural and physiological traits on A in this study, a path analysis was conducted (Fig. 7). We found direct impacts of g<sub>s</sub> and P<sub>minor</sub> on A, with path values of 0.426 and 0.390, respectively. However, no significant or direct effects of g<sub>m</sub> or X<sub>major</sub> on A were observed (Fig. 7). X<sub>major</sub> was found to have direct effects on g<sub>s</sub> and g<sub>m</sub> with path values of 0.876 and 0.615, respectively. Moreover, X<sub>major</sub> was found to be correlated with P<sub>minor</sub>, although the causal relationship between them was not clear. Therefore, the result suggested an indirect influence of X<sub>major</sub> on A via g<sub>s</sub> and P<sub>minor</sub>. Collectively, our present data could explain 37.8, 76.7 and 93.2 %, respectively, of the variations in g<sub>m</sub>, g<sub>s</sub> and A (Fig. 7).

Relationships between leaf structural traits among rice genotypes

In this study, we found that LMA was positively correlated with LT, but not with LD (Table 4). Leaf thickness was positively correlated with X<sub>major</sub>, X<sub>minor</sub>, P<sub>major</sub> and P<sub>minor</sub>, and was negatively correlated with LD among rice genotypes (Table 4). Additionally, X<sub>major</sub>, X<sub>minor</sub>, P<sub>major</sub> and P<sub>minor</sub> were all positively correlated with each other (Table 4).

DISCUSSION

The effects of X<sub>major</sub> on g<sub>s</sub> in rice plants

In the present study, leaf xylem sizes (X<sub>major</sub> and X<sub>minor</sub>) were found to be positively correlated with g<sub>s</sub>, K<sub>leaf</sub> and A (Fig. 2); and X<sub>major</sub> was found to have a direct impact on g<sub>s</sub> (Fig. 7). These findings are in agreement with our first hypothesis that a large xylem size benefits leaf hydraulic conductance, stomatal conductance and thus photosynthesis. To the best of our knowledge, this is the first study investigating the relationship between leaf photosynthesis and leaf xylem size in rice plants.

Water diffusion through xylem conduits is suggested to follow the Hagen–Poiseuille equation, K<sub>x</sub> = ∑<sub>i=1</sub><sup>N</sup> (πd<sub>i</sub><sup>4</sup>/128η) (Nobel, 2009; North et al., 2013), where N is the number of tracheids in each vein multiplied by the number of veins in the leaf, d is the diameter of tracheid and η is the viscosity of water. We may infer from this equation that large xylem conduits should be more important than small xylem conduits in determining K<sub>x</sub>

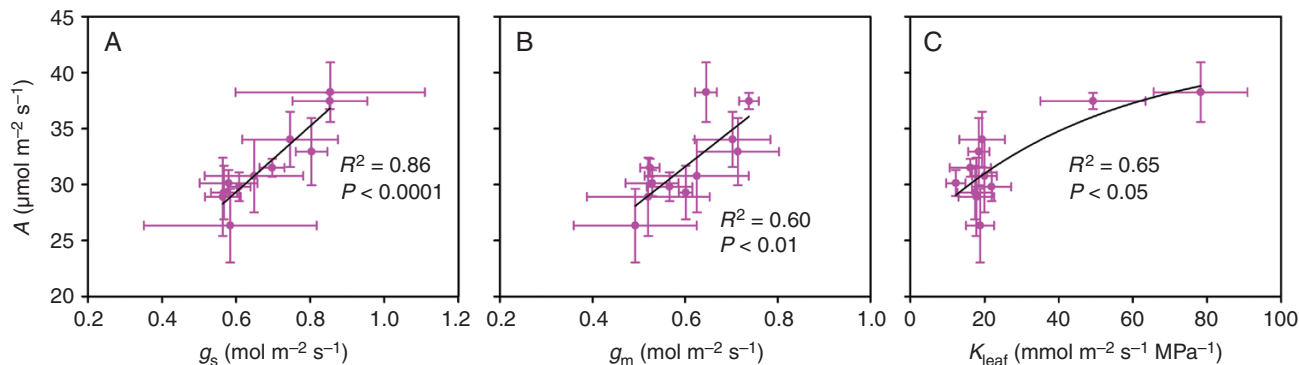


FIG. 1. Relationships between leaf photosynthetic rate ( $A$ ) and stomatal conductance ( $g_s$ ), mesophyll conductance ( $g_m$ ) and leaf hydraulic conductance ( $K_{\text{leaf}}$ ). The data points are the means  $\pm$  s.d. of 3–5 biological replicates for  $A$ ,  $g_s$  and  $g_m$ , and of 4–8 biological replicates for  $K_{\text{leaf}}$ . Both linear and non-linear models were fitted, and the models with the lowest residual sum of squares are shown. Model equations: (A)  $A = 29.5g_s + 11.7$ , (B)  $A = 32.6g_m + 12.1$  and (C)  $A = 16.9(1 - e^{-0.02K_{\text{leaf}}}) + 25.3$ .

and in turn  $K_{\text{leaf}}$ . This would explain why  $X_{\text{major}}$ , but not  $X_{\text{minor}}$ , had a significant influence on  $g_s$  and  $A$  in the path analysis (Fig. 7). Nevertheless, the correlation between  $A$  and  $X_{\text{major}}$  was significantly decreased when controlling  $X_{\text{minor}}$  (Table 3), which suggested that the correlation between  $X_{\text{major}}$  and leaf physiological traits (including  $K_{\text{leaf}}$  and  $A$ ) may also be partly driven by a developmental constraint that ties  $X_{\text{major}}$  to  $X_{\text{minor}}$  (Table 4). There may be some confusion about the high values of  $K_{\text{leaf}}$  observed in YY12 and YY2640 (Table 1). However, we would like to note that guttation was only observed in these two genotypes after dark adaptation overnight, and this is consistent with the high  $\Psi_{\text{leaf}}$  ( $-0.14$  MPa in YY12 and  $-0.09$  MPa in YY2640) found in these two genotypes after  $K_{\text{leaf}}$  measurements.

In fact, leaf vein traits have been frequently found to be related to  $K_{\text{leaf}}$  (Brodrribb *et al.*, 2007; Brodrribb and Field, 2010; Brodrribb and Jordan, 2011) and thus  $g_s$  (Boyce *et al.*, 2009; Brodrribb and Jordan, 2011). Inside leaves, water first flows through leaf xylem and then through the tissues outside the xylem, both of which are related to leaf morphological and anatomical traits (Buckley *et al.*, 2015; Xiong *et al.*, 2017). More densely packed leaf veins can provide more parallel water flow paths through the vein system (Buckley *et al.*, 2015), and can shorten the distance from leaf veins to stomata (Brodrribb *et al.*, 2007). Therefore,  $K_{\text{leaf}}$  is frequently found to be positively correlated with leaf vein density (Sack and Frolle, 2006; Brodrribb *et al.*, 2007; Brodrribb and Field, 2010), and to be negatively correlated with the IVDs (Brodrribb and Jordan, 2011). In the present study, however,  $K_{\text{leaf}}$  was found to be positively correlated with  $X_{\text{major}}$  (Fig. 2C) but not with IVDs (Supplementary data Fig. S4). In a previous study,  $K_{\text{leaf}}$  was found to be positively correlated with  $IVD_{\text{minor}}$  in 11 cultivated and wild rice plants (Xiong *et al.*, 2015), which contradicts the previous hypothesis that more leaf veins can lead to a larger  $K_{\text{leaf}}$ . Thus, both the study of Xiong *et al.* (2015) and the present study suggested that leaf vein density is not the major determinant of  $K_{\text{leaf}}$  in rice plants, and leaf xylem size is a more promising target trait than leaf vein density in manipulation of  $K_{\text{leaf}}$  and thus  $g_s$  in rice plants.

Intraspecific variation in  $g_s$  was not correlated with either stomatal size or density in the present study (Supplementary data Fig. S5), which is in agreement with previous studies (Xiong *et al.*, 2017; Zhang *et al.*, 2019). This suggested that

stomatal aperture is more important than stomatal morphology in determining  $g_s$  in rice plants. In contrast to the intraspecific variation in  $g_s$ , interspecific variation in  $g_s$  may be positively correlated with stomatal density and/or the ratio of stomatal densities between the adaxial and abaxial leaf surface (Franks and Beerling, 2009; Xiong and Flexas, 2020).

#### The effects of $X_{\text{major}}$ on $g_m$ in rice plants

In this study, we found that  $X_{\text{major}}$  was positively correlated with  $g_m$  (Fig. 2B), which has not been reported in previous studies. However, the mechanisms underlying the correlation are not known. We speculated that larger major xylems might be associated with more mesophyll cell layers between the upper and lower epidermis, which may consequently lead to a larger mesophyll cell area and thus a larger chloroplast surface area facing the intercellular airspace (Hanba *et al.*, 1999). Further research is needed in this area to study the mechanism underlying the correlation between  $X_{\text{major}}$  and  $g_m$ .

#### The effects of $P_{\text{minor}}$ on $A$ in rice plants

Leaf phloem sizes ( $P_{\text{major}}$  and  $P_{\text{minor}}$ ) were found to be positively correlated with  $g_s$ ,  $K_{\text{leaf}}$  and  $A$  (Fig. 3); and  $P_{\text{minor}}$  had a direct impact on leaf photosynthesis (Fig. 7). These results support our second hypothesis that leaf phloem size is positively correlated with leaf photosynthetic rate.

In  $C_3$  plants, leaf photosynthesis is limited by stomatal conductance, mesophyll conductance, leaf biochemical capacities and the utilization of photoassimilates (Paul and Foyer, 2001; Ainsworth and Bush, 2011; Tanaka *et al.*, 2013; Simkin *et al.*, 2017; Xu *et al.*, 2019). The transport capacity of carbohydrates is closely related to leaf vein structures (Flora and Madore, 1996; Stewart *et al.*, 2019). There are several studies that provide evidence that the responses of leaf phloem structures and photosynthesis to various growth conditions are tightly coordinated (Adams *et al.*, 2007, 2013, 2016). These studies are consistent with our present findings that a larger  $P_{\text{minor}}$  was directly associated with a higher leaf photosynthetic rate among rice genotypes (Fig. 7), which may be due to the increased phloem

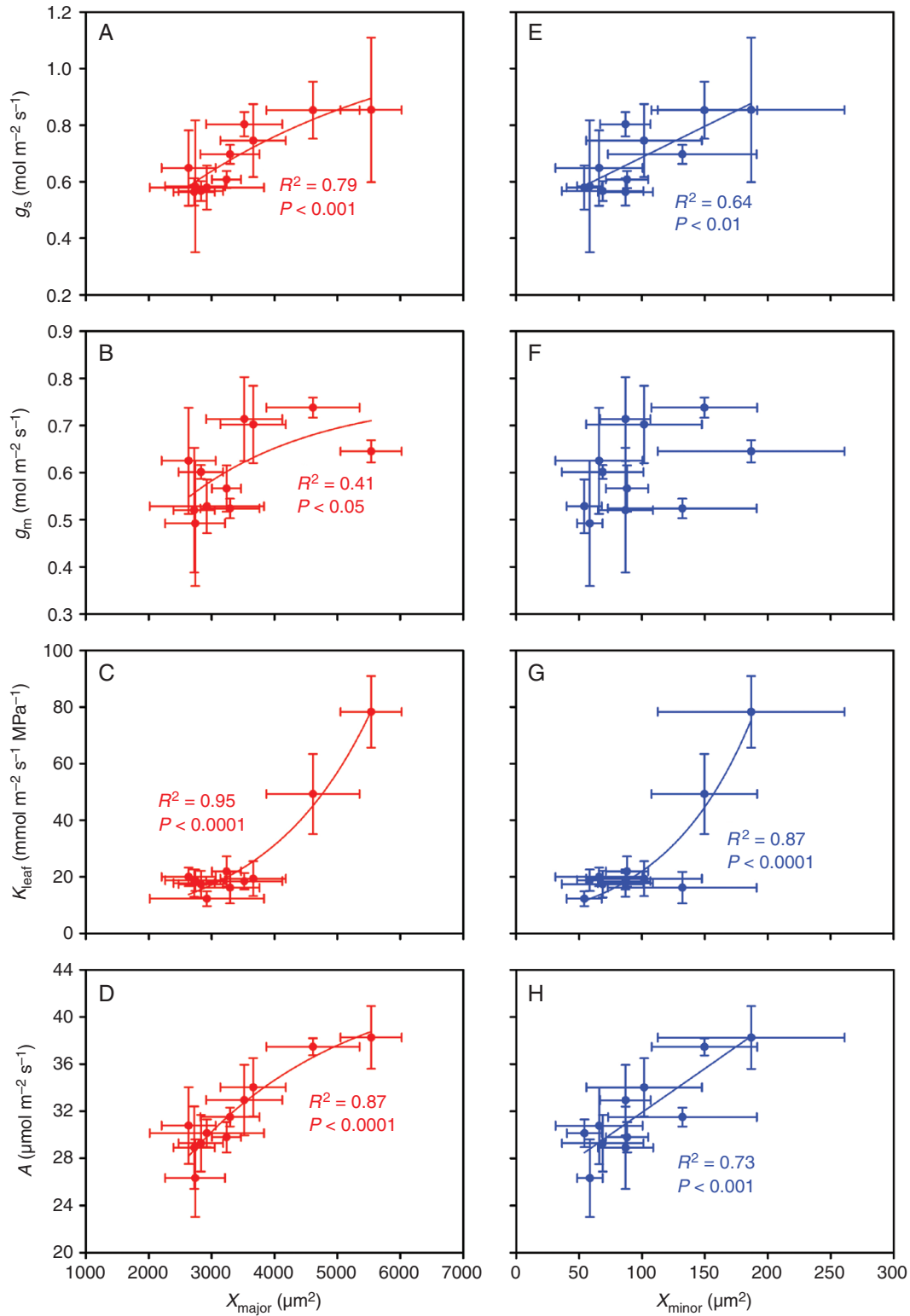


FIG. 2. Relationships between total area of xylem conduits per major and per minor veins ( $X_{\text{major}}$  and  $X_{\text{minor}}$ ) and  $g_s$ ,  $g_m$ ,  $K_{\text{leaf}}$  and  $A$ . The data points are the means  $\pm$  s.d. of 3–5 biological replicates for  $X_{\text{major}}$ ,  $X_{\text{minor}}$ ,  $A$ ,  $g_s$  and  $g_m$ , and of 4–8 biological replicates for  $K_{\text{leaf}}$ . Both linear and non-linear models were fitted, and the model with the lowest residual sum of squares is shown. Model equations: (A)  $g_s = 1.16(1 - e^{-0.0003X_{\text{major}}})$ , (B)  $g_m = 0.76(1 - e^{-0.0005X_{\text{major}}})$ , (C)  $K_{\text{leaf}} = 2.83e^{0.0006X_{\text{major}}}$ , (D)  $A = 43.7(1 - e^{-0.0004X_{\text{major}}})$ , (E)  $g_s = 0.0022X_{\text{minor}} + 0.47$ , (G)  $K_{\text{leaf}} = 5.3e^{0.0142X_{\text{minor}}}$  and (H)  $A = 0.0745X_{\text{minor}} + 24.5$ .  $X_{\text{major}}$ , xylem area per major vein;  $X_{\text{minor}}$ , xylem area per minor area;  $g_s$ , stomatal conductance;  $g_m$ , mesophyll conductance;  $K_{\text{leaf}}$ , leaf hydraulic conductance; and  $A$ , leaf photosynthetic rate.

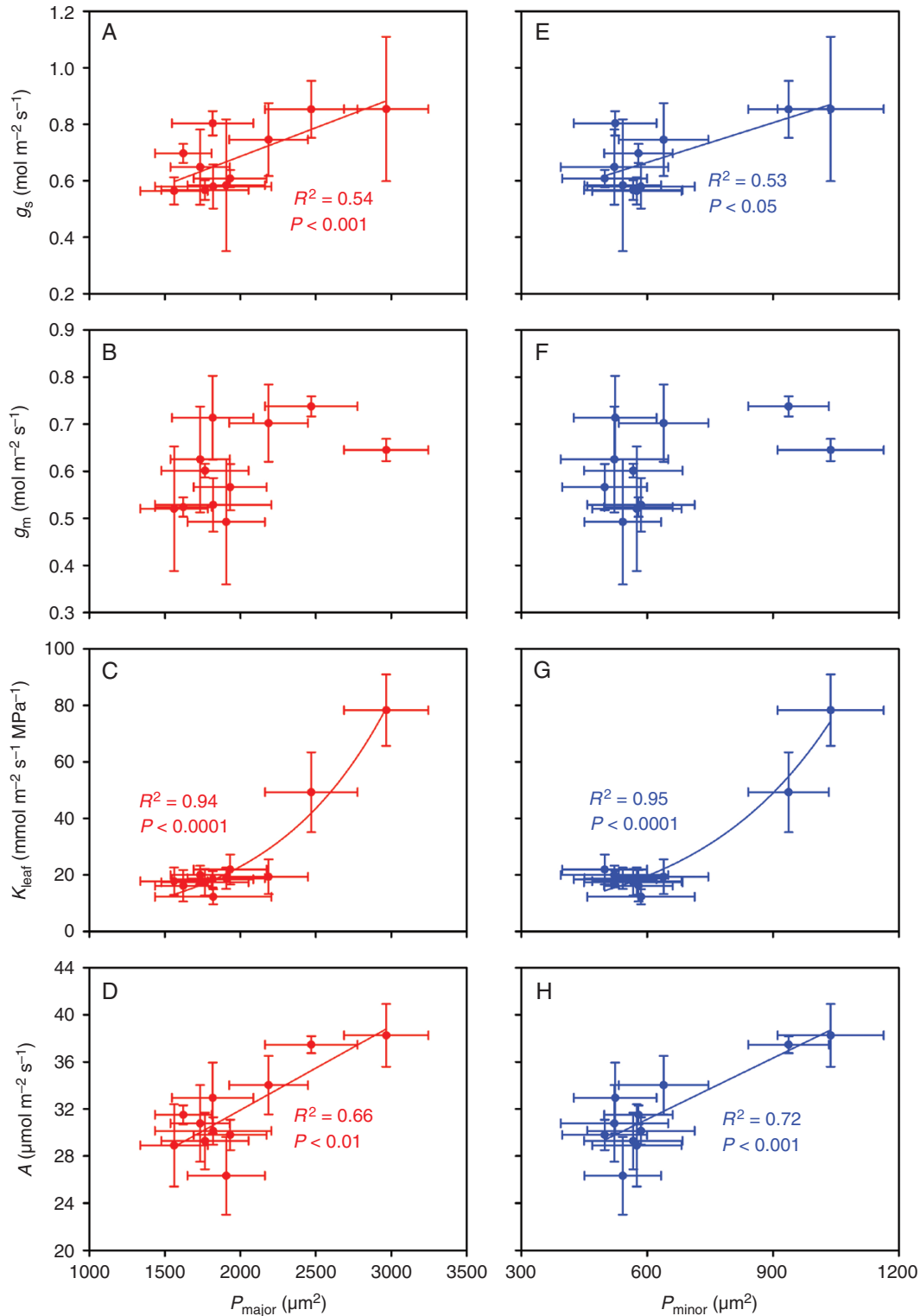


FIG. 3. Relationships between leaf phloem area per major and per minor veins ( $P_{\text{major}}$  and  $P_{\text{minor}}$ ) and  $g_s$ ,  $g_m$ ,  $K_{\text{leaf}}$  and  $A$ . The data points are the means  $\pm$  s.d. of 3–5 biological replicates for  $P_{\text{major}}$ ,  $P_{\text{minor}}$ ,  $A$ ,  $g_s$  and  $g_m$ , and of 4–8 biological replicates for  $K_{\text{leaf}}$ . Both linear and non-linear models were fitted, and the models with the lowest residual sum of squares are shown. Model equations: (A)  $g_s = 0.0002P_{\text{major}} + 0.28$ , (C)  $K_{\text{leaf}} = 1.78e^{0.0013P_{\text{major}}}$ , (D)  $A = 0.0071P_{\text{major}} + 17.7$ , (E)  $g_s = 0.0005P_{\text{minor}} + 0.38$ , (G)  $K_{\text{leaf}} = 3.15e^{0.003P_{\text{minor}}}$  and (H)  $A = 0.0173P_{\text{minor}} + 20.7$ .  $P_{\text{major}}$ , phloem area per major vein;  $P_{\text{minor}}$ , phloem area per minor vein;  $g_s$ , stomatal conductance;  $g_m$ , mesophyll conductance;  $K_{\text{leaf}}$ , leaf hydraulic conductance; and  $A$ , leaf photosynthetic rate.



loading capacity. Consistently, in rice plants, mutant lines with increased leaf vein density were associated with the enhanced capacity for triose phosphate utilization, which was suggested to be related to the improved photoassimilate transport capacity (Feldman *et al.*, 2017). In fact, most of the mesophyll cells inside leaves are closer to minor phloem than major phloem

(Supplementary data Fig. S1). Therefore, it is no surprise that we only observed a significant impact of  $P_{\text{minor}}$  on leaf photosynthesis because transport capacity of carbohydrates from mesophyll cells to sink tissues may be largely dependent on minor phloem (Sack and Scoffoni, 2013).

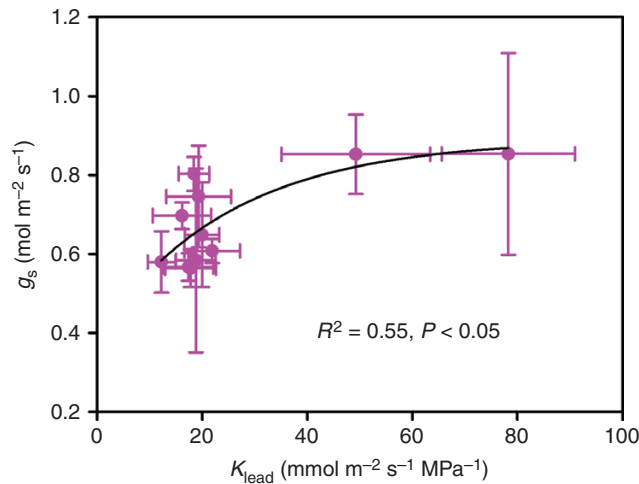


FIG. 4. Relationships between leaf hydraulic conductance ( $K_{\text{leaf}}$ ) and stomatal conductance ( $g_s$ ). The data points are the means  $\pm$  s.d. of 3–5 biological replicates for  $g_s$  and of 4–8 biological replicates for  $K_{\text{leaf}}$ . Both linear and non-linear models were fitted, and the model with the lowest residual sum of squares is shown. Model equation:  $g_s = 0.5(1 - e^{-0.04K_{\text{leaf}}}) + 0.39$ .

#### The effects of LT and LMA on A in rice plants

Leaf thickness was found to be positively correlated with  $X_{\text{major}}$ ,  $X_{\text{minor}}$ ,  $P_{\text{major}}$  and  $P_{\text{minor}}$  (Table 4); and it was also found to be positively correlated with  $g_s$ ,  $K_{\text{leaf}}$  and A (Fig. 5). These results support our third hypothesis that leaf thickness is correlated with leaf xylem and phloem sizes, and thus gas exchange parameters. However, the correlation between leaf thickness and photosynthesis was also significant when  $g_s$  was controlled (Table 3). This suggested that the influence of leaf thickness on photosynthesis is only partially correlated with  $g_s$  and  $K_{\text{leaf}}$ . In fact, there have been many studies showing higher leaf nitrogen and chlorophyll contents in thicker leaves (Peng, 2000; Han *et al.*, 2019; Reddy *et al.*, 2020), which can result in a higher A.

The positive correlation between leaf thickness and  $K_{\text{leaf}}$  was consistent with a previous study in rice plants (Xiong *et al.*, 2015). The study of Xiong *et al.* (2015) hypothesized that thicker leaves may have more parallel flow pathways outside the xylem and consequently result in a higher  $K_{\text{leaf}}$ . In the present study, however, we suggested that the positive correlation between leaf thickness and  $K_{\text{leaf}}$  may be related to the co-ordination between leaf structures, because leaf thickness

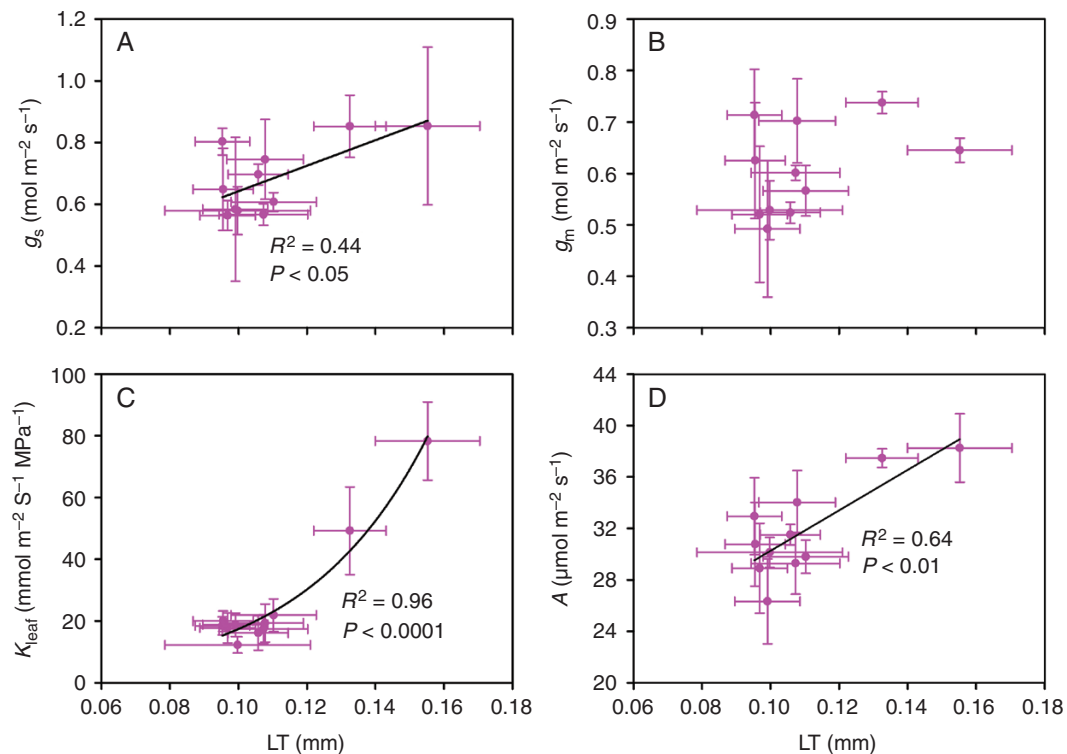


FIG. 5. Relationships between leaf thickness (LT) and stomatal conductance ( $g_s$ ), mesophyll conductance ( $g_m$ ), leaf hydraulic conductance ( $K_{\text{leaf}}$ ) and leaf photosynthetic rate (A). The data points are the means  $\pm$  s.d. of 3–5 biological replicates for LT,  $g_s$ ,  $g_m$  and A, and of 4–8 biological replicates for  $K_{\text{leaf}}$ . Both linear and non-linear models were fitted, and the models with the lowest residual sum of squares are shown. Model equations: (A)  $g_s = 4.14\text{LT} + 0.229$ , (C)  $K_{\text{leaf}} = 1.1e^{27.6\text{LT}}$  and (D)  $A = 157\text{LT} + 14.5$ .

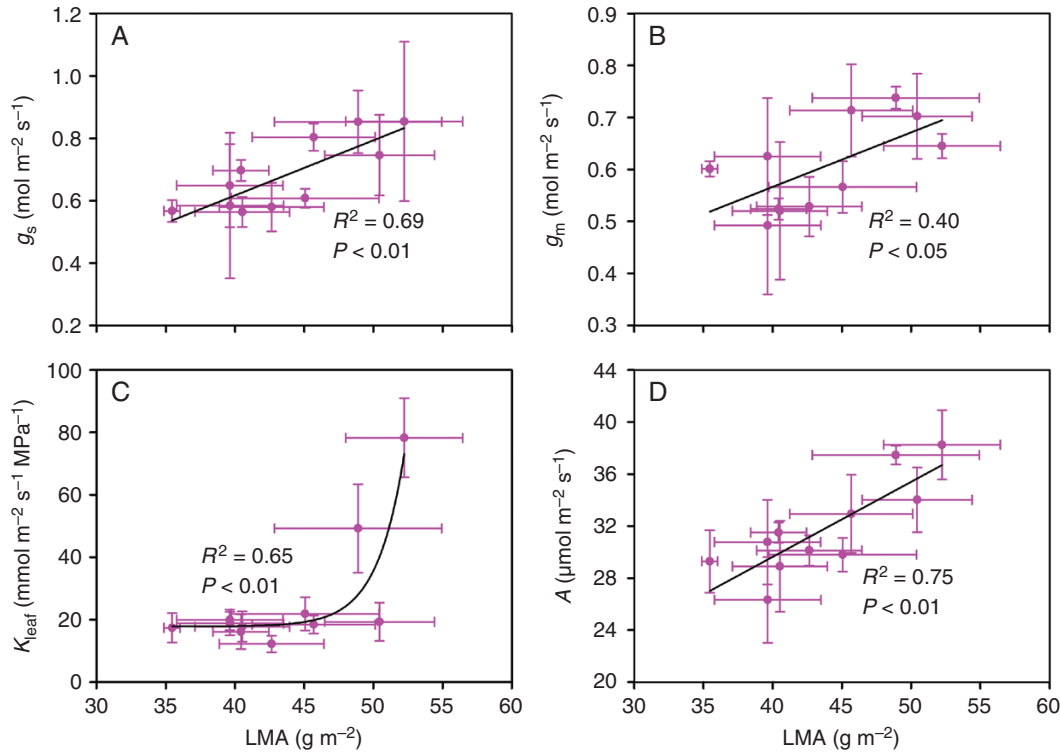


FIG. 6. Relationships between leaf mass per area (LMA) and stomatal conductance ( $g_s$ ), mesophyll conductance ( $g_m$ ), leaf hydraulic conductance ( $K_{leaf}$ ) and leaf photosynthetic rate ( $A$ ). The data points are the means  $\pm$  s.d. of 3–5 biological replicates for LT,  $g_s$ ,  $g_m$  and  $A$ , and 4–8 biological replicates for  $K_{leaf}$ . Both linear and non-linear models were fitted, and the model with the lowest residual sum of squares is shown. Model equations: (A)  $g_s = 0.0177LMA - 0.0897$ , (B)  $g_m = 0.0105LMA + 0.1470$ , (C)  $K_{leaf} = 1.73^{-10}e^{0.5071LMA} + 17.86$  and (D)  $A = 0.5773LMA + 6.5377$ .

TABLE 3. Partial correlations (Pearson's  $r$ ) between leaf photosynthetic rate ( $A$ ) and the related physiological and structural traits

	A									
$g_m$	<b>0.78**</b>	/	0.15	<b>0.79**</b>	<b>0.75*</b>	<b>0.88**</b>	<b>0.69*</b>	<b>0.81**</b>	<b>0.83**</b>	
$g_s$	<b>0.93***</b>	<b>0.81**</b>	/	<b>0.86**</b>	<b>0.68*</b>	<b>0.79**</b>	<b>0.84**</b>	<b>0.86**</b>	<b>0.89**</b>	
$K_{leaf}$	<b>0.80**</b>	<b>0.81**</b>	0.55	/	-0.38	0.24	0.19	-0.02	0.17	
$X_{major}$	<b>0.92***</b>	<b>0.91***</b>	<b>0.64*</b>	<b>0.81**</b>	/	<b>0.66*</b>	<b>0.78**</b>	<b>0.67*</b>	<b>0.82**</b>	
$X_{minor}$	<b>0.86**</b>	<b>0.92***</b>	0.51	0.56	0.08	/	0.62	0.46	0.54	
$P_{major}$	<b>0.81**</b>	<b>0.74*</b>	0.53	0.34	-0.32	0.48	/	0.19	0.32	
$P_{minor}$	<b>0.85**</b>	<b>0.87**</b>	<b>0.70*</b>	0.51	0.01	0.44	0.47	/	0.49	
LT	<b>0.80**</b>	<b>0.85**</b>	<b>0.66*</b>	0.21	-0.44	0.19	0.20	-0.01	/	
Control variables	Zero-order	$g_m$	$g_s$	$K_{leaf}$	$X_{major}$	$X_{minor}$	$P_{major}$	$P_{minor}$	LT	

\* $P < 0.05$ ,

\*\* $P < 0.01$ ,

\*\*\* $P < 0.001$ .  $g_m$ , mesophyll conductance;  $g_s$ , stomatal conductance;  $K_{leaf}$ , leaf hydraulic conductance;  $X_{major}$ , total area of xylem conduits per major vein;  $X_{minor}$ , total area of xylem conduits per minor vein;  $P_{major}$ , phloem area per major vein;  $P_{minor}$ , phloem area per minor vein; and LT, leaf thickness.

was highly correlated with  $X_{major}$  (Table 4). In contrast to the positive correlation between leaf thickness and  $K_{leaf}$  found in the present study and the study of Xiong *et al.* (2015), the studies of Brodrribb *et al.* (2007) and Brodrribb and Field (2010) found a negative relationship between  $K_{leaf}$  and vein–epidermal distance (VED), where VED is generally positively related to leaf thickness, among different plant species. They hypothesized that a longer distance for H<sub>2</sub>O to diffuse from leaf veins to the epidermis can potentially result in a higher diffusion resistance and a lower  $K_{leaf}$  (Brodrribb *et al.*, 2007; Brodrribb and Field, 2010). Therefore, the correlation between leaf thickness and  $K_{leaf}$  may be species dependent.

The present study showed that LMA was positively correlated with LT,  $g_s$ ,  $g_m$ ,  $K_{leaf}$  and  $A$  (Table 4; Fig. 6). These results support the previous hypothesis that LMA is positively related to leaf photosynthesis if leaf thickness determines the variation of LMA. However, the finding that LMA was positively correlated with leaf thickness but not with leaf density (Table 4) is inconsistent with our previous study (Xiong *et al.*, 2016) which was also conducted in rice plants. Xiong *et al.* (2016) found that LMA is determined more by leaf density than leaf thickness, which is similar to the findings in the study of Poorter *et al.* (2009) which investigated various different plant species. The different results regarding the determinant of LMA may relate

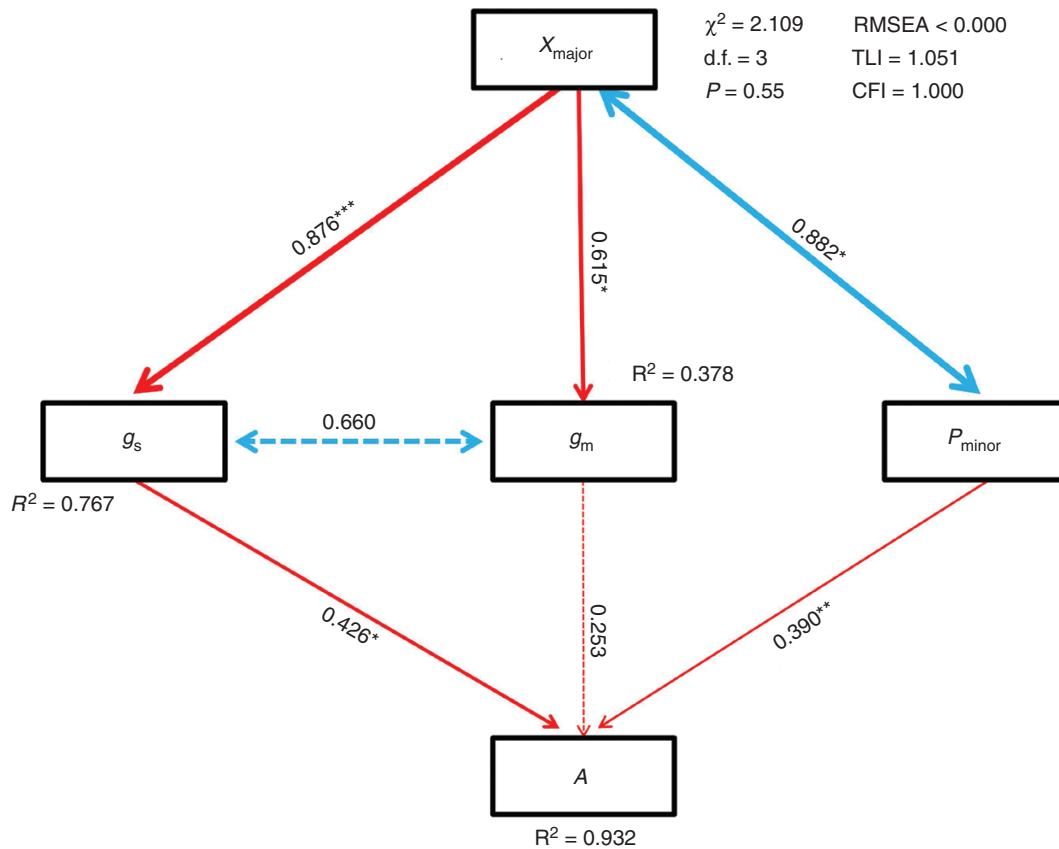


FIG. 7. Path analysis model for the effect of  $X_{major}$ ,  $P_{minor}$ ,  $g_s$  and  $g_m$  on  $A$ . Arrows represent pathways among variables. Significant values are indicated by \* ( $P < 0.05$ ), \*\* ( $P < 0.01$ ) and \*\*\* ( $P < 0.001$ ).  $R^2$  values are indicated for the dependent variables. Double arrowed lines represent correlation without establishment of causality.  $X_{major}$ , total area of xylem conduits per major vein;  $P_{minor}$ , leaf phloem area per minor vein;  $g_s$ , stomatal conductance;  $g_m$ , mesophyll conductance;  $A$ , leaf photosynthetic rate.

TABLE 4. Linear Pearson correlation matrix of leaf structural traits

	LMA	LT	LD	$X_{major}$	$X_{minor}$	$P_{major}$	$P_{minor}$	$S_{major}$	$S_{minor}$
LMA	1								
LT	<b>0.674*</b>	1							
LD	0.156	<b>-0.618*</b>	1						
$X_{major}$	<b>0.841**</b>	<b>0.934***</b>	-0.348	1					
$X_{minor}$	<b>0.694*</b>	<b>0.878***</b>	-0.453	<b>0.916***</b>	1				
$P_{major}$	<b>0.814**</b>	<b>0.929***</b>	-0.368	<b>0.932***</b>	<b>0.765**</b>	1			
$P_{minor}$	<b>0.690*</b>	<b>0.940***</b>	-0.515	<b>0.924***</b>	<b>0.861**</b>	<b>0.906***</b>	1		
$S_{major}$	<b>0.823**</b>	<b>0.920***</b>	-0.360	<b>0.983***</b>	<b>0.900***</b>	<b>0.924***</b>	<b>0.908***</b>	1	
$S_{minor}$	<b>0.716*</b>	<b>0.963***</b>	-0.531	<b>0.950***</b>	<b>0.939***</b>	<b>0.884***</b>	<b>0.931***</b>	<b>0.915***</b>	1

\* $P < 0.05$ ,

\*\* $P < 0.01$ ,

\*\*\* $P < 0.001$ . LMA, leaf mass per area; LT, leaf thickness; LD, leaf density;  $X_{major}$ , total area of xylem conduits per major vein;  $X_{minor}$ , total area of xylem conduit per minor vein;  $P_{major}$ , phloem area per major vein;  $P_{minor}$ , phloem area per minor vein;  $S_{major}$ , vascular bundle area of major vein; and  $S_{minor}$ , vascular bundle area of minor vein among rice genotypes.

to the differing genotypes. Several wild relatives of rice plants were used in the study of Xiong *et al.* (2016), while only cultivated rice plants were examined in the present study. This suggested that the determinant of LMA is complex, and is species and/or genotypic dependent.

Perspective for future crop breeding

Improving photosynthesis is considered as one of the most important approaches to further increase crop yield in the future (Zhu *et al.*, 2010; Long *et al.*, 2015). Our present study suggested that leaf xylem size could be used as a new targeted

trait during rice breeding to further increase photosynthesis via improving  $K_{\text{leaf}}$ ,  $g_s$  and  $g_m$  (Fig. 2). The improvement of leaf photosynthesis may not necessarily increase crop yield if the utilization of photoassimilates is limited (Flexas, 2016). Interestingly, our results indicated that minor phloem size is a promising target to increase the transport capacity of carbohydrates from mesophyll cells to sink tissues (Fig. 7). Therefore, the manipulation of vascular bundles, which consists of both xylem and phloem conduits, is a promising approach to improve photosynthesis in rice plants (Table 4; Fig. 7; Supplementary data Fig. S2). However, we would like to note that the impacts of both leaf xylem and phloem sizes on crop photosynthesis and yield should be further studied under field conditions, which should be more relevant for crop breeding programmes.

### Conclusion

This study provided the first evidence for the important role of  $X_{\text{major}}$  and  $P_{\text{minor}}$  in leaf photosynthesis in rice plants.  $P_{\text{minor}}$  had a direct impact on leaf photosynthesis, and  $X_{\text{major}}$  had an indirect impact on leaf photosynthesis via  $g_s$  and  $P_{\text{minor}}$ . The influence of leaf thickness on photosynthesis may be partly related to the co-ordination between leaf thickness and leaf xylem and phloem sizes.

### SUPPLEMENTARY DATA

Supplementary data are available online at <https://academic.oup.com/aob> and consist of the following. Table S1: species of 11 rice genotypes used in this study. Figure S1: diagram illustrating details of the leaf anatomical traits measured in Shanyou 63. Figure S2: relationships between leaf photosynthetic rate and intercellular  $\text{CO}_2$  concentration and chloroplast  $\text{CO}_2$  concentration. Figure S3: relationships between vascular bundle area and  $g_s$ ,  $g_m$ ,  $K_{\text{leaf}}$  and A. Figure S4: relationships between interveinal distance and  $g_s$ ,  $g_m$ ,  $K_{\text{leaf}}$  and A. Figure S5: relationships between the effect of stomatal conductance and stomatal size and density on both abaxial and adaxial leaf surfaces.

### ACKNOWLEDGEMENTS

Y.L. and G.H. conceived and designed the research. G.H. and Y.S. conducted the experiments and collected the data. Y.L. and G.H. analysed the data and wrote the paper. S.P. commented on and revised the paper.

### FUNDING

This research was supported by the National Natural Science Foundation of China (31871532 and 32172103) and by the Fundamental Research Funds for the Central Universities (2021ZKPY017).

### CONFLICT OF INTEREST

The authors declare that they have no known competing financial interests or personal relationships that could have appeared to influence the work reported in this paper.

### LITERATURE CITED

- Adams WW, Watson AM, Mueh KE, et al. 2007. Photosynthetic acclimation in the context of structural constraints to carbon export from leaves. *Photosynthesis Research* **94**: 455–466.
- Adams WW, Cohu CM, Muller O, Demmig-Adams B. 2013. Foliar phloem infrastructure in support of photosynthesis. *Frontiers in Plant Science* **4**: 194. doi:10.3389/fpls.2013.00194.
- Adams WW, Stewart JJ, Cohu CM, Muller O, Demmig-Adams B. 2016. Habitat temperature and precipitation of *Arabidopsis thaliana* ecotypes determine the response of foliar vasculature, photosynthesis, and transpiration to growth temperature. *Frontiers in Plant Science* **7**: 1026. doi:10.3389/fpls.2016.01026.
- Ainsworth EA, Bush DR. 2011. Carbohydrate export from the leaf: a highly regulated process and target to enhance photosynthesis and productivity. *Plant Physiology* **155**: 64–69. doi:10.1104/pp.110.167684.
- Barbour MM, Evans JR, Simonin K, Caemmerer SV. 2016. Online  $\text{CO}_2$  and  $\text{H}_2\text{O}$  oxygen isotope fractionation allows estimation of mesophyll conductance in  $\text{C}_4$  plants, and reveals that mesophyll conductance decreases as leaves age in both  $\text{C}_4$  and  $\text{C}_3$  plants. *New Phytologist* **210**: 875–889. doi:10.1111/nph.13830.
- Bernacchi CJ, Portis AR, Nakano H, Caemmerer SV, Long SP. 2002. Temperature response of mesophyll conductance. Implications for the determination of Rubisco enzyme kinetics and for limitations to photosynthesis in vivo. *Plant Physiology* **130**: 1992–1998.
- Boyce CK, Brodrribb TJ, Field TS, Zwieniecki MA. 2009. Angiosperm leaf vein evolution was physiologically and environmentally transformative. *Proceedings of the Royal Society B: Biological Sciences* **276**: 1771–1776.
- Brodrribb TJ. 2009. Xylem hydraulic physiology: the functional backbone of terrestrial plant productivity. *Plant Science* **177**: 245–251. doi:10.1016/j.plantsci.2009.06.001.
- Brodrribb TJ, Field TS. 2010. Leaf hydraulic evolution led a surge in leaf photosynthetic capacity during early angiosperm diversification. *Ecology Letters* **13**: 175–183.
- Brodrribb TJ, Jordan GJ. 2011. Water supply and demand remain balanced during leaf acclimation of *Nothofagus cunninghamii* trees. *New Phytologist* **192**: 437–448. doi:10.1111/j.1469-8137.2011.03795.x.
- Brodrribb TJ, Field T, Jordan GJ. 2007. Leaf maximum photosynthetic rate and venation are linked by hydraulics. *Plant Physiology* **144**: 1890–1898.
- Brodrribb TJ, Jordan G, Carpenter RJ. 2013. Unified changes in cell size permit coordinated leaf evolution. *New Phytologist* **199**: 559–570. doi:10.1111/nph.12300.
- Buckley TN. 2005. The control of stomata by water balance. *New Phytologist* **168**: 275–292.
- Buckley TN, John GP, Scoffoni C, Sack L. 2015. How does leaf anatomy influence water transport outside the xylem? *Plant Physiology* **168**: 1616–1635. doi:10.1104/pp.15.00731.
- Evans JR, von Caemmerer SV. 2013. Temperature response of carbon isotope discrimination and mesophyll conductance in tobacco. *Plant, Cell & Environment* **36**: 745–756.
- Evans JR, Sharkey TD, Berry JA, Farquhar GD. 1986. Carbon isotope discrimination measured concurrently with gas exchange to investigate  $\text{CO}_2$  diffusion in leaves of higher plants. *Functional Plant Biology* **13**: 281–292. doi:10.1071/pp9860281.
- Farquhar GD, Cernusak LA. 2012. Ternary effects on the gas exchange of isotopologues of carbon dioxide. *Plant, Cell & Environment* **35**: 1221–1231. doi:10.1111/j.1365-3040.2012.02484.x.
- Farquhar GD, Richards RA. 1984. Isotopic composition of plant carbon correlates with water-use efficiency of wheat genotypes. *Functional Plant Biology* **11**: 539–552. doi:10.1071/pp9840539.
- Feldman AB, Leung H, Baraoidan M, et al. 2017. Increasing leaf vein density via mutagenesis in rice results in an enhanced rate of photosynthesis, smaller cell sizes and can reduce interveinal mesophyll cell number. *Frontiers in Plant Science* **8**: 1883.
- Flexas J. 2016. Genetic improvement of leaf photosynthesis and intrinsic water use efficiency in  $\text{C}_3$  plants: why so much little success? *Plant Science* **251**: 155–161.
- Flexas J, Scoffoni C, Gago J, Sack L. 2013. Leaf mesophyll conductance and leaf hydraulic conductance: an introduction to their measurement and co-ordination. *Journal of Experimental Botany* **64**: 3965–3981. doi:10.1093/jxb/ert319.
- Flexas J, Clemente-Moreno MJ, Bota J, et al. 2021. Cell wall thickness and composition are involved in photosynthetic limitation. *Journal of Experimental Botany* **72**: 3971–3986.
- Flora LL, Madore MA. 1996. Significance of minor-vein anatomy to carbohydrate transport. *Planta* **198**: 171–178.



- Franks PJ, Beerling DJ. 2009. Maximum leaf conductance driven by CO<sub>2</sub> effects on stomatal size and density over geologic time. *Proceedings of the National Academy of Sciences, USA* **106**: 10343–10347. doi:10.1073/pnas.0904209106.
- Franks PJ, Farquhar GD. 2007. The mechanical diversity of stomata and its significance in gas-exchange control. *Plant Physiology* **143**: 78–87.
- Grace JB, Anderson TM, Olf H, Scheiner SM. 2010. On the specification of structural equation models for ecological systems. *Ecological Monographs* **80**: 67–87. doi:10.1890/09-0464.1.
- Guy RD, Fogel M, Berry JA. 1993. Photosynthetic fractionation of the stable isotopes of oxygen and carbon. *Plant Physiology* **101**: 37–47. doi:10.1104/pp.101.1.37.
- Han JM, Zhang YJ, Lei ZY, Zhang WF, Zhang YL. 2019. The higher area-based photosynthesis in *Gossypium hirsutum* L. is mostly attributed to higher leaf thickness. *Photosynthetica* **57**: 420–427. doi:10.32615/ps.2019.052.
- Hanba YT, Miyazawa S, Terashima I. 1999. The influence of leaf thickness on the CO<sub>2</sub> transfer conductance and leaf stable carbon isotope ratio for some evergreen tree species in Japanese warm-temperate forests. *Functional Ecology* **13**: 632–639. doi:10.1046/j.1365-2435.1999.00364.x.
- Hanba YT, Kogami H, Terashima I. 2002. The effect of growth irradiance on leaf anatomy and photosynthesis in *Acer* species differing in light demand. *Plant, Cell & Environment* **25**: 1021–1030. doi:10.1046/j.1365-3040.2002.00881.x.
- Hassiotou F, Renton M, Ludwig M, Evans JR, Veneklaas EJ. 2010. Photosynthesis at an extreme end of the leaf trait spectrum: how does it relate to high leaf dry mass per area and associated structural parameters? *Journal of Experimental Botany* **61**: 3015–3028. doi:10.1093/jxb/erq128.
- John GP, Scoffoni C, Sack L. 2013. Allometry of cells and tissues within leaves. *American Journal of Botany* **100**: 1936–1948. doi:10.3732/ajb.1200608.
- Krapp A, Stitt M. 1995. An evaluation of direct and indirect mechanisms for the ‘sink-regulation’ of photosynthesis in spinach: changes in gas exchange, carbohydrates, metabolites, enzyme activities and steady-state transcript levels after cold-girdling source leaves. *Planta* **195**: 313–323.
- Long SP, Marshall-Colon A, Zhu XG. 2015. Meeting the global food demand of the future by engineering crop photosynthesis and yield potential. *Cell* **161**: 56–66. doi:10.1016/j.cell.2015.03.019.
- Lu Z, Ren T, Li J, et al. 2020. Nutrition-mediated cell and tissue-level anatomy triggers the covariation of leaf photosynthesis and leaf mass per area. *Journal of Experimental Botany* **71**: 6524–6537.
- McKown AD, Cochard H, Sack L. 2010. Decoding leaf hydraulics with a spatially explicit model: principles of venation architecture and implications for its evolution. *The American Naturalist* **175**: 447–460. doi:10.1086/650721.
- Nardini AGE, Salleo S. 2005. Hydraulic efficiency of the leaf venation system in sun- and shade-adapted species. *Functional Plant Biology* **32**: 953–961.
- Niinemets U. 1999. Research review. Components of leaf dry mass per area – thickness and density – alter leaf photosynthetic capacity in reverse directions in woody plants. *New Phytologist* **144**: 35–47. doi:10.1046/j.1469-8137.1999.00466.x.
- Nobel PS. 2009. *Physicochemical and environmental plant physiology*, 4th edn. San Diego, CA: Academic Press.
- North GB, Lynch FH, Maharaj FD, Phillips CA, Woodside WT. 2013. Leaf hydraulic conductance for a tank bromeliad: axial and radial pathways for moving and conserving water. *Frontiers in Plant Science* **4**: 78.
- Paul MJ, Foyer CH. 2001. Sink regulation of photosynthesis. *Journal of Experimental Botany* **52**: 1383–1400. doi:10.1093/jexbot/52.360.1383.
- Peng S. 2000. Single-leaf and canopy photosynthesis of rice. *Studies in Plant Science* **7**: 213–228.
- Poorter H, Niinemets U, Poorter L, Wright IJ, Villar R. 2009. Causes and consequences of variation in leaf mass per area (LMA): a meta-analysis. *New Phytologist* **182**: 565–588. doi:10.1111/j.1469-8137.2009.02830.x.
- Reddy SH, Singhal RK, DaCosta MVJ, et al. 2020. Leaf mass area determines water use efficiency through its influence on carbon gain in rice mutants. *Physiologia Plantarum* **169**: 194–213.
- Sack L, Frole K. 2006. Leaf structural diversity is related to hydraulic capacity in tropical rain forest trees. *Ecology* **87**: 483–491. doi:10.1890/05-0710.
- Sack L, Scoffoni C. 2012. Measurement of leaf hydraulic conductance and stomatal conductance and their responses to irradiance and dehydration using the Evaporative Flux Method (EFM). *Journal of Visualized Experiment* **70**: e4179.
- Sack L, Scoffoni C. 2013. Leaf venation: structure, function, development, evolution, ecology and applications in the past, present and future. *New Phytologist* **198**: 983–1000. doi:10.1111/nph.12253.
- Scoffoni C, Chatelet DS, Pasquet-Kok J, et al. 2016. Hydraulic basis for the evolution of photosynthetic productivity. *Nature Plants* **2**: 1–8.
- Sharkey TD. 1985. Photosynthesis in intact leaves of C<sub>3</sub> plants: physics, physiology and rate limitations. *The Botanical Review* **51**: 53–105. doi:10.1007/bf02861058.
- Simkin AJ, Lopez-Calcagno PE, Davey PA, et al. 2017. Simultaneous stimulation of sedoheptulose 1,7-bisphosphatase, fructose 1,6-bisphosphate aldolase and the photorespiratory glycine decarboxylase-H protein increases CO<sub>2</sub> assimilation, vegetative biomass and seed yield in *Arabidopsis*. *Plant Biotechnology Journal* **15**: 805–816.
- Stewart JJ, Muller O, CoHu CM, Demmig-Adams B, Adams WW. 2019. Quantification of leaf phloem anatomical features with microscopy. *Methods in Molecular Biology* **2014**: 55–72.
- Sugiura D, Terashima I, Evans JR. 2020. A decrease in mesophyll conductance by cell-wall thickening contributes to photosynthetic downregulation. *Plant Physiology* **183**: 1600–1611.
- Tanaka Y, Sugano SS, Shimada T, Hara-Nishimura I. 2013. Enhancement of leaf photosynthetic capacity through increased stomatal density in *Arabidopsis*. *New Phytologist* **198**: 757–764.
- Tcherkez G, Schaeufele R, Nogués S, et al. 2010. On the <sup>13</sup>C/<sup>12</sup>C isotopic signal of day and night respiration at the mesocosm level. *Plant, Cell & Environment* **33**: 900–913.
- Wishart J. 1928. The generalised product moment distribution in samples from a normal multivariate population. *Biometrika* **3**: 2–52.
- Xiong D, Flexas J. 2020. From one side to two sides: the effects of stomatal distribution on photosynthesis. *New Phytologist* **228**: 1754–1766. doi:10.1111/nph.16801.
- Xiong D, Yu T, Zhang T, Li Y, Peng S, Huang J. 2015. Leaf hydraulic conductance is coordinated with leaf morpho-anatomical traits and nitrogen status in the genus *Oryza*. *Journal of Experimental Botany* **66**: 741–748. doi:10.1093/jxb/eru434.
- Xiong D, Flexas J, Yu T, Peng S, Huang J. 2017. Leaf anatomy mediates coordination of leaf hydraulic conductance and mesophyll conductance to CO<sub>2</sub> in *Oryza*. *New Phytologist* **213**: 572–583.
- Ye M, Zhang Z, Huang G, Xiong Z, Peng S, Li Y. 2020. High leaf mass per area *Oryza* genotypes invest more leaf mass to cell wall and show a low mesophyll conductance. *AoB Plants* **12**: plaa028. doi:10.1093/aob/pla028.
- Zhang C, Turgeon R. 2009. Downregulating the sucrose transporter VpSUT1 in *Verbascum phoeniceum* does not inhibit phloem loading. *Proceedings of the National Academy of Sciences, USA* **106**: 18849–18854. doi:10.1073/pnas.0904189106.
- Zhang Q, Peng S, Li Y. 2019. Increase rate of light-induced stomatal conductance is related to stomatal size in the genus *Oryza*. *Journal of Experimental Botany* **70**: 5259–5269.
- Zhu XG, Long S, Ort DR. 2010. Improving photosynthetic efficiency for greater yield. *Annual Review of Plant Biology* **61**: 235–261.